ISSN 1974-9821
Vol. 4 N. 3
June 2011

International Review on Modelling and Simulations (IREMOS)

PART A

Contents:

(continued on inside back cover)

Praise Worthy Prize

International Review on Modelling and Simulations (IREMOS)

The ***International Review on Modelling and Simulations (IREMOS)*** is a publication of the **Praise Worthy Prize S.r.l..**
The Review is published bimonthly, appearing on the last day of February, April, June, August, October, December.

Published and Printed in Italy by **Praise Worthy Prize S.r.l.,** Naples, June 30, 2011.

Praise Worthy Prize

International Review on Modelling and Simulations (I.RE.MO.S.), Vol. 4, N. 3
June 2011

Operational Analysis of 2.3kV Neutral Point Clamped, Series Connected H-Bridge and Auxiliary Series Connected H-Bridge Five-Level Converters

M. Niakinezhad[1], M. A. Akbari Baseri[2], S. S. Fazel[3], A. Mehdipour[4]

Abstract – *This paper discuss a Five-Level Neutral Point Clamped Voltage Source Converter (5L-NPC VSC), a Five-Level Series Connected H-Bridge Voltage Source Converter (5L-SCHB VSC), and a new Five-Level Auxiliary Series Connected H-Bridge Voltage Source Converter (5L-ASCHB VSC) on the basis of the state-of-the-art 3.3kV, and 1.7kV IGBTs for a 2.3kV Medium Voltage Converter (MVC). To derive specific converter characteristics of the aforementioned topologies the power semiconductors utilization, the installed switch power, the converter losses, the semiconductor loss distribution, efficiency, the harmonic spectra, and material costs are discussed in details. Matlab/Simulink is used as a simulation tool for analysis and comparison.*

Keywords: *Five-level Converters, Medium Voltage Drives, Power Electronics*

I. Introduction

Drive manufacturers (e.g. ABB, Converteam, Siemens, and Robicon) offer different topologies of voltage source converter for medium power industrial applications. High Voltage IGBTs (HV-IGBTs) and Integrated Gate Commutated Thyristors (IGCTs) are mainly applied to Neutral Point Clamped- and Flying Capacitor Voltage Source Converters (NPC- and FLC VSCs) 1.2kV and 1.7kV Low Voltage IGBTs (LV-IGBTs) are usually used in Series Connected H-Bridge Voltage Source Converters (SCHB VSCs). This class of Multi-Level Converter (MLC) is a popular power converter for motor drives [1-4], power supplies [5], [6], and ac power systems [7-10]. MLCs popularity increased due to their excellent efficiency, high power density, low output harmonies, low commutation losses, high reliability [11], and reduction in the commutation frequency [12], [13]. The expenses of semiconductors and passive components, converter losses, modulation schemes and harmonic spectra were compared for 2.3kV industrial medium voltage drives [11], [12]. This paper also includes a new Auxiliary Series Connected H-Bridge Voltage Source Converter (ASCHB VSC) [13], [14], [15] for 2.3kV medium voltage drives (Fig. 1) which realizes the considerable reduction in the number of main power switches and uses no more diodes or capacitors in comparison with SCHB VSC. State-of-the-art 3.3kV and 1.7kV HV-IGBTs are assumed. The design of the semiconductors, the converter losses, semiconductor loss distribution, efficiency and the harmonic spectra are described in details to derive specific converter characteristics of the aforementioned topologies.

II. Basic Structure and Function of Five-Level Auxiliary H-Bridge (5L-ASCHB) Voltage Source Converter (VSC)

This section describes the basic structure of 5L-ASCHB-VSC topology. This class of multi-level converter is based on a new connection of single-phase converter (Figs. 1), and lately is introduced by [13].

Figs. 1 show the basic topology of the 5L-ASCHB VSC used for the implementation of new SCHB VSC.

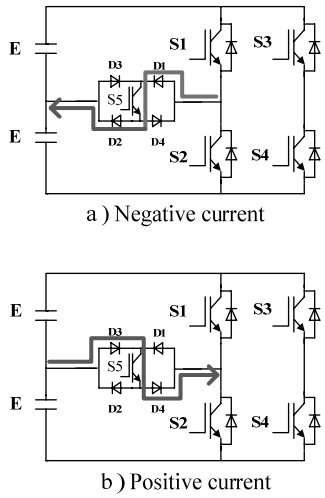

Figs. 1. Five-Level Auxiliary H-Bridge (5L-ASCHB)

Each converter legs consist of two active switches and two freewheeling diodes in anti-parallel with each switch. The auxiliary switch consists of an IGBT and four diodes connected between middle point of DC link and the first

Manuscript received and revised May 2011, accepted June 2011

leg according to Figs. 1. The switching states in this model are similar to SCHB power cell which introduced in previous literature (Table I).

TABLE I
SWITCHING STATES OF FIVE-LEVEL AUXILIARY H-BRIDGE (5L-ASCHB)

Vo	S1	S2	S3	S4	S5
2E	1	0	0	1	0
E	0	0	0	1	1
0	0	1	0	1	0
0	1	0	1	0	0
-E	0	0	1	0	1
-2E	0	1	1	0	0

If S1 and S4 are turn on simultaneously, the output voltage will be 2*E*, while the output voltage is -2*E* when S3 and S2 both have on state. To generate the zero output voltage, two upper switches (S1 and S3) or two lower switches (S2 and S4) should be turned on. In order to prevent a short circuit, two switches in each leg shouldn't be turned on simultaneously. The *E* and *–E* voltage levels can be generated by applying the switch S5. If S5 and S4 have on state, the output voltage will be *E*, while the voltage *–E* can be generated when S5 and S3 both have on state. For the positive and negative phase current, (D3, D4) and (D1, D2) are on respectively. These states are visualized in Figs. 1.

III. Basic of Comparison

The circuit configurations of the 5L-NPC VSC, the 5L-SCHB VSC, and the 5L-ASCHB VSC are illustrated in Figs. 2.

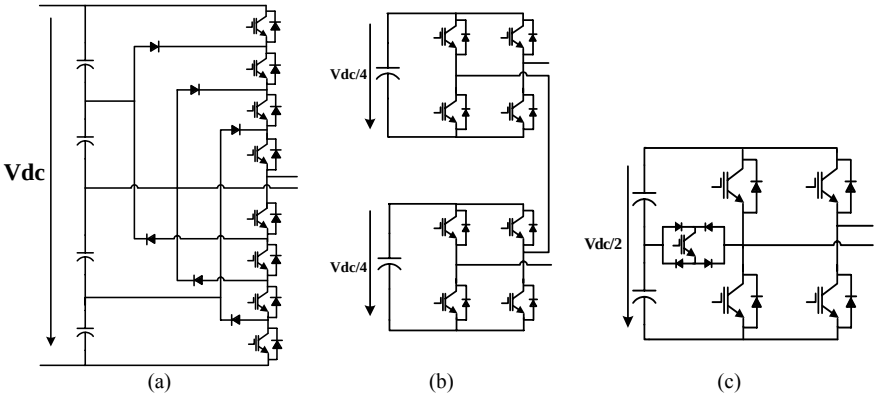

Figs. 2. One phase of the five-level topologies ($E=V_{dc,n}/4$)
a) 5L-NPC; b) 5L-SCHB; c) 5L-ASCHB VSCs

Table II presents the characteristics converter data for the comparison of aforementioned topologies. The phase current I_{ph}, the converter output power S_C and the carrier frequency f_C of the modulation are varied in order to compare converter losses, semiconductor loss distribution, harmonic spectra, and efficiency of converters.

Table III represents the characteristics of the power semiconductors for converters with V_{ll}=2.3 kV output voltage and maximum junction temperature of $T_{j,max}$=125ºC at phase current of I_{ph}=600 A and carrier frequency of f_C=750 Hz. An important criterion of the device reliability is the ratio between the commutation voltage (V_{com}) and device commutation voltage for a device reliability of 100FIT due to cosmic radiation ($V_{com@100FIT}$ is equivalent to one failure in 10^7 operation hours for a typical junction temperature of 25 ºC).

Dc-link voltage to achieve an output line-to-line voltage 2.3 kV is calculated by:

$$V_{dc,n} = \sqrt{2} V_{ll,1,rms} \times 1.08 \qquad (1)$$

III.1. Loss Approximation Based on Datasheets

A loss model of the device is developed based on an experimental determination of the power losses. The total power losses in the converter are estimated to determine the junction temperature and categorized into two following losses that will introduced in the following.

TABLE II
CONVERTER DATA FOR THE COMPARISON

Nominal dc-link voltage $V_{dc,n}$	3383 V
Phase current ($I_{ph,rms}$)	600 A-785 A
Apparent output power (S_C)	2.39 MVA-3.13 MVA
Type of modulation	SPWM with third harmonic
Carrier frequency (f_C)	750 Hz-3845 Hz
Output line-to-line voltage ($V_{ll,rms,1}$)	2.3 kV
Output frequency (f)	50 Hz
Maximum junction temperature $T_{j,max}$ (IGBT, diode)	125 ºC

TABLE III
POWER SEMICONDUCTOR DESIGN FOR $V_{ll,rms,1}$ =2.3kV; I_{ph}=600A; f_c=750Hz

\	5L-NPCVSC	5L-SCHB VSC	5L-ASCHB VSC	
Required dc-link voltage	3383 V (V_{dc})	846 V (V_{dc}/4)	1692 V (V_{dc}/2)	
Commutation voltage (V_{com})	846 V		Main	1692 V
			Aux.	846 V
Rated device voltage ($V_{CE,n}$)	1700 V		Main	3300 V
			Aux.	1700 V
$V_{com@100FIT}$	900 V		Main	1800 V
			Aux.	900 V
$V_{com}/V_{com@100FIT}$	0.94			
Rated IGBT current ($I_{C,n}$) $T_{j,max}$=125 C	612.5 A	618 A	Main	668 V
			Aux.	537 V
Installed switch power (S_S)	46.85 MVA	37.82 MVA	47.89 MVA	

III.1.1. Conduction Losses

The conduction losses $P_{cond,x}$ of an IGBT or a diode can be expressed by the well-known approximation:

$$P_{cond,x} = \frac{1}{T} \cdot \sum_{t=0}^{T} \left(V_{on,x} + A_{cond,x} \cdot i_x(t)^{B_{cond,x}} \right) \cdot i_x(t) \cdot t_s \quad (2)$$

where $P_{cond,x}$ is the conduction loss in device *x, T* is the fundamental period, $V_{on,x}$ is on state voltage parameter for device *x,* $A_{cond,x}$ and $B_{cond,x}$ are the curve-fitted constants for device *x* and $i_x(t)$ is the instantaneous value of the device current.

III.1.2. Switching Losses

Switching losses are created by the commutation processes between different switch states. These commutation processes can be classified into (1) natural or inductive commutations, which are characterized by turn-on losses of active switches and recovery losses of diodes, and (2) forced or capacitive commutations, which are contrarily characterized by turn-off losses of active switches. Turn-on losses of diodes are usually small and can be neglected [16], [17]. It is possible to calculate the switching losses on the basis of the collector-emitter voltage and the collector current. However, this is not a very accurate method because of the need of rough approximations. Therefore, it is more effective and more accurate to measure the switching losses directly as a function of the load current and then describe the relationship with a simple equation:

$$P_{sw,x} = \frac{1}{T} \sum_{t=0}^{T} \left(A_{on,x} \cdot i_x(t)^{B_{on,x}} + A_{off,x} \cdot i_x(t)^{B_{off,x}} \right) \frac{V_{com}}{V_{ce}} \quad (3)$$

where $P_{sw,x}$ is the average switching losses for device *x*, $A_{on,x}$, $B_{on,x}$ and $A_{off,x}$, $B_{off,x}$ are turn-on and turn-off curve-fitting constants for device *x* respectively, V_{com} is the commutation voltage, and V_{ce} denotes the voltage at which the losses were measured.

This equation is useful for turn-on and turn-off losses of the IGBT as well as for the diode. The constant parameters are determined by applying a first-order curve-fitting of the measured on state voltage characteristics and the switching losses which are depending on the load current. The fitting parameters and thermal resistances of the semiconductors which are considered in this paper are given in Table IV, where the abbreviations *T* (IGBT) and *D* (Diode) are used for device *x*.

TABLE IV
FITTING PARAMETERS AND THERMAL RESISTANCES OF MEDIUM VOLTAGE IGBTS/DIODES

IGBT Module	FZ600R17KE3 EUPEC 1.7 kV/600 A	FZ800R33KF2C EUPEC 3.3 kV/800 A
V_{CE}	900 V	1800 V
$V_{on,T}$	0.7 V	1 V
$V_{on,D}$	0.5 V	0.8 V
$A_{on,T}$	0.00057942	0.000959466
$B_{on,T}$	0.9351	1.115444805
$A_{off,T}$	0.00066378	0.003771589
$B_{off,T}$	0.88671	0.841860719
$A_{off,D}$	0.0088387	0.059062305
$B_{off,D}$	0.43627	0.422711861
$A_{cond,T}$	0.010357	0.033603338
$B_{cond,T}$	0.79806	0.687596711
$A_{cond,D}$	0.050265	0.015314298
$B_{cond,D}$	0.52041	0.725344373
$R_{th-jc,T}$	0.04	0.013
$R_{th-jc,D}$	0.065	0.026
$R_{th-ch,T}$	0.016	0.009
$R_{th-ch,D}$	0.026	0.018

The total semiconductor losses of each IGBT or Diode are derived from:

$$P_{loss,x} = P_{cond,x} + P_{sw,x} \quad (4)$$

For safe operation, the power losses generated by each module must be dissipated. At the steady state, the junction temperature T_j can be calculated by using the following thermal equation:

$$T_{j,x} = P_{loss,x} \cdot \left(R_{th-jc,x} + R_{th-ch,x} \right) \quad (5)$$

R_{th-jc} denotes the thermal resistance of the IGBT/diode from junction to case and R_{th-ch} is the thermal resistance of the IGBT/diode from case to heat-sink. To determine the ideal current rating of each semiconductor device ($I_{C,n}$), the occurring device losses in the worst case operating point, the maximum junction temperature $T_{j,max}$=125°C, and the thermal resistances of the considered IGBTs and diodes in the module are assumed.

The comparisons are based on the IGBTs and diodes datasheets and the simulation of semiconductor losses in [18]. To calculate the ideal current rating $I_{C,n}$, an ideal parallel connection of the commercially available devices is considered. The calculated ideal rated devices currents $I_{C,n}$ ensure that the junction temperature of the mostly stressed device reaches a value of $T_{j,max}$ = 125°C in one of the worst case of six critical operating points (OP) [11]. The thermal resistance of commercially available devices depends on the rational number of ideally parallel connected modules according to the silicon area and the module size. The temperature of the heat-sink is assumed constant (T =80°C).

The required current rating to achieve an output current of I_{ph}=600 A is different due to various power semiconductors, circuit structures, and modulation schemes in aforementioned topologies. The voltage utilization of the semiconductors is the same in all converter topologies. The installed switch power determined with ($S_s=V_{CE,n}.I_{C,n}.n+0.5V_{RPM}.I_{C,n}.k$) where n and k are the number of IGBTs and diodes respectively. The installed switch power of the 5L-ASCHB VSC is higher than other topologies (Table III).

IV. Comparison and Results

To compare the converter topologies for variety of applications three different conditions are assumed.

IV.1. Loss Comparison with Constant S_s and f_c

At the first step, the installed switch power and the carrier frequency are assumed S_s=47.89 MVA and f_C=750Hz respectively for all considered converter topologies. These assumptions make possible to evaluate maximum output power of converters (S_C). Maximum output power is achieved when one of the IGBTs or diodes in each topology in one of the six critical points reaches maximum junction temperature $T_{j,max}$=125°C.

The maximum output power in 5L-SCHB VSC reaches 3.03 MVA which is increased by 27% and 24% higher than in comparison with 5L-ASCHB VSC and 5L-NPC VSC respectively (Table V).

Also the converter losses of the 5L-NPC VSC are 15% and 7% lower than 5L-ASCHB VSC and 5L-SCHB VSC respectively (Fig. 3).

TABLE V
MAXIMUM PHASE CURRENT AND APPARENT OUTRUT POWER FOR
S_S=47.89 MVA; f_C=750 Hz; $T_{j,max}$=125 °C

Topology	5L-NPC VSC	5L-SCHB VSC	5L-ASCHB VSC	
Installed switch power (S_S)	47.89 MVA			
Rated IGBT current ($I_{C,n}$)	626 A	782.5 A	Main	668 A
			Aux.	537 A
Maximum phase current $I_{ph,max}$	613 A	760 A	600 A	
Maximum apparent output power ($S_{C,max}$)	2.44 MVA	3.03 MVA	2.39 MVA	

During one period of carrier signal in the 5L-NPC VSC one commutation occurs while in the 5L-SCHB VSC two commutations occur. Also, the switching losses of the 5L-ASCHB VSC are higher than 5L-SCHB VSC and 5L-NPC VSC, due to the usage of 3.3kV IGBTs that generate clearly more switching losses than the 1.7kV IGBTs at their corresponding commutation voltage. The converter losses, the semiconductor loss distribution, and the harmonic spectra of considered topologies are illustrated in Figs. 3-5 respectively.

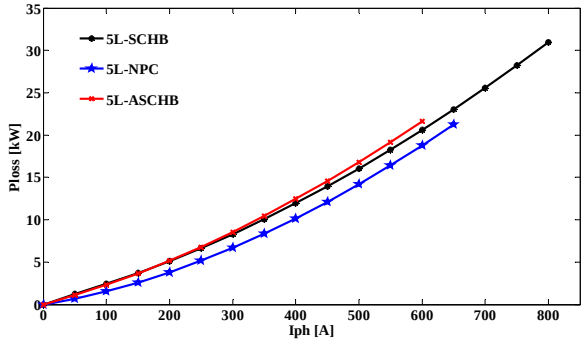

Fig. 3. Total converter losses as a function of phase current
(f_c =750Hz; f =50Hz; m_a=1.15; cosφ = 0.9)

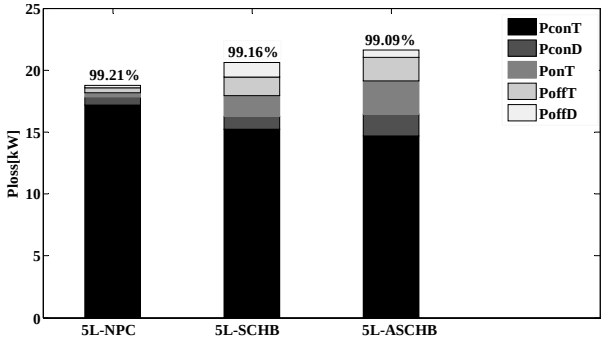

Fig. 4. Loss distribution of semiconductor and converter efficiency
(f_c =750Hz; f =50Hz; m_a=1.15; cosφ = 0.9; I_{ph}=600A)

According to Figs. 5 the first carrier band of line to line output voltage frequency of 5L-SCHB VSC is centered around quadruple of the carrier frequency, while the first carrier of 5L-ASCHB VSC and 5L-NPC VSC are the same and centered around the carrier frequency.

Therefore, the output filter of 5L-SCHB VSC can be distinctly smaller than corresponding filter of the 5L-NPC, and 5L-ASCHB VSCs. The THD and WTHD of three converters are listed in Table VI. The THD of 5L-NPC, and 5L-ASCHB VSCs are equal while the THD of

5L-SCHB VSC is 6.2% higher than the two other topologies. The 5L-SCHB VSC has the lowest WTHD in comparison with the other topologies.

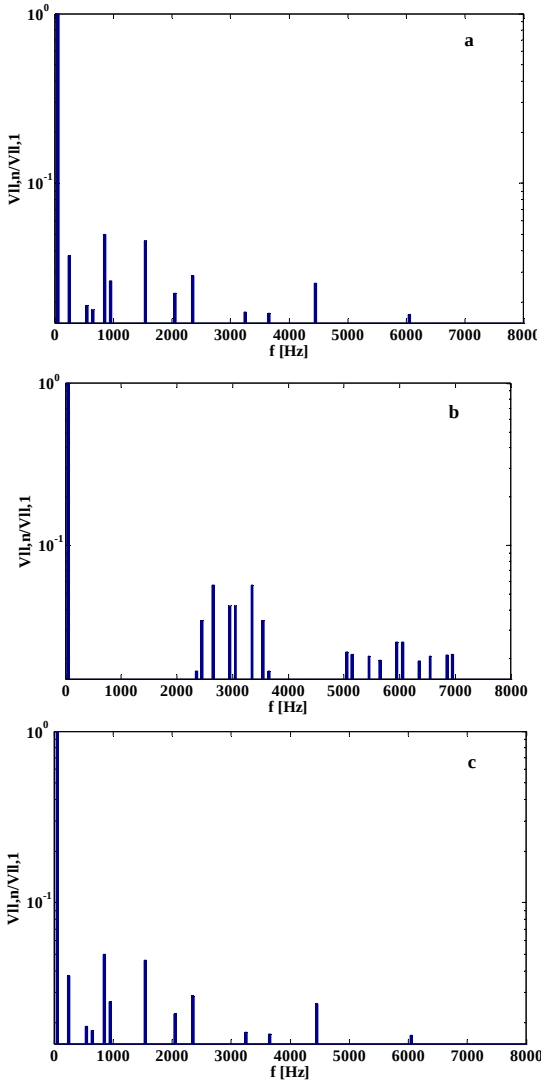

Figs. 5. Harmonic spectra of line-to-line voltage V_{ll}
(f_c=750Hz, f=50Hz, m_a=1.15)
a) 5L-NPC VSC; b) 5L-SCHB VSC; c) 5L-ASCHB VSC

IV.2. Maximum Carrier Frequency with Constant S_S and S_C

At this section a constant installed switch power (S_s=47.89 MVA) as well as a same output current (I_{ph}=600 A) and converter output power (S_c =2.39 MVA) are considered to evaluate the maximum carrier frequency of the aforementioned topologies. The maximum carrier frequency should be evaluated based on the losses of the maximally stressed device ($T_{j,max}$=125°C) in one of the six critical operating points for the thermal design. The 5L-SCHB VSC can have the highest possible carrier frequency as shown in Table VII.

Losses, semiconductor loss distribution and harmonic spectra of the converters are shown in Figs. 6-8 respectively. The 5L-SCHB VSC generates the minimum total losses for carrier frequency up to 250Hz.

However, in the range of 250Hz to 930Hz the 5L-NPC VSC has the lowest total losses compared to other topologies. The maximum possible carrier frequency in 5L-SCHB VSC is much higher than other topologies due to uniform semiconductor loss distribution.

Table VIII shows that the 5L-SCHB VSC has the highest THD in maximum possible carrier frequency and lower WTHD compared to the other topologies.

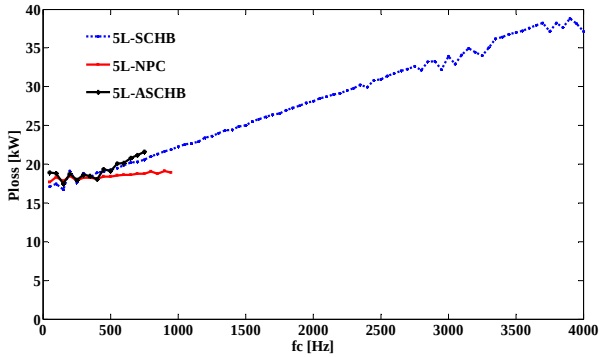

Fig. 6. Total converter losses as a function of frequency
($f_{C,5L-NPC}$=930Hz; $f_{C,5L-SCHB}$=3850Hz; $f_{C,5L-ASCHB}$=750Hz; I_{ph}=600A; f=50Hz; m_a=1.15; cosφ = 0.9)

TABLE VI
THD AND WTHD OF LINE-TO-LINE OUTPUT VOLTAGE
f_c=750Hz; m_a=1.15

Topology	THD	WTHD
5L-NPC VSC	17.5 %	0.77 %
5L-SCHB VSC	23.7 %	0.20 %
5L-ASCHB VSC	17.5 %	0.77 %

TABLE VII
MAXIMUM CARRIER FREQUENCY; S_s=47.89 MVA; S_c=2.39 MVA; I_{ph}=600 A; $T_{j,max}$=125 °C

Topology	5L-NPC VSC	5L-SCHB VSC	5L-ASCHB VSC
Installed switch power (S_S)		47.89 MVA	
Maximum apparent output power ($S_{C,max}$)		2.39 MVA	
Phase current (I_{ph})		600 A	
Rated IGBT current ($I_{C,n}$)	626 A	782 A	Main 668 A Aux. 537 A
Maximum carrier frequency (f_c)	928 Hz	3845 Hz	750 Hz

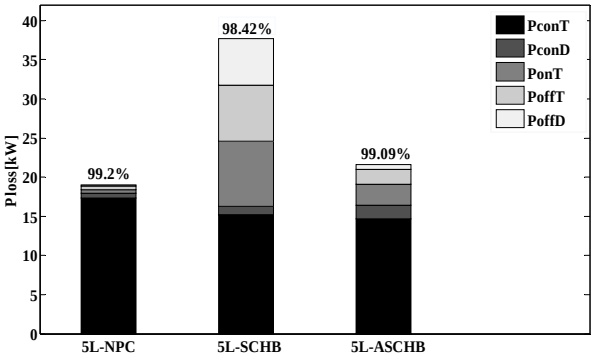

Fig. 7. Loss distribution of semiconductor and converter efficiency ($f_{C,5L\text{-}NPC}$=930Hz; $f_{C,5L\text{-}SCHB}$=3850Hz; $f_{C,5L\text{-}ASCHB}$=750Hz; f=50Hz; m_a=1.15; cosφ = 0.9, I_{ph}=600A)

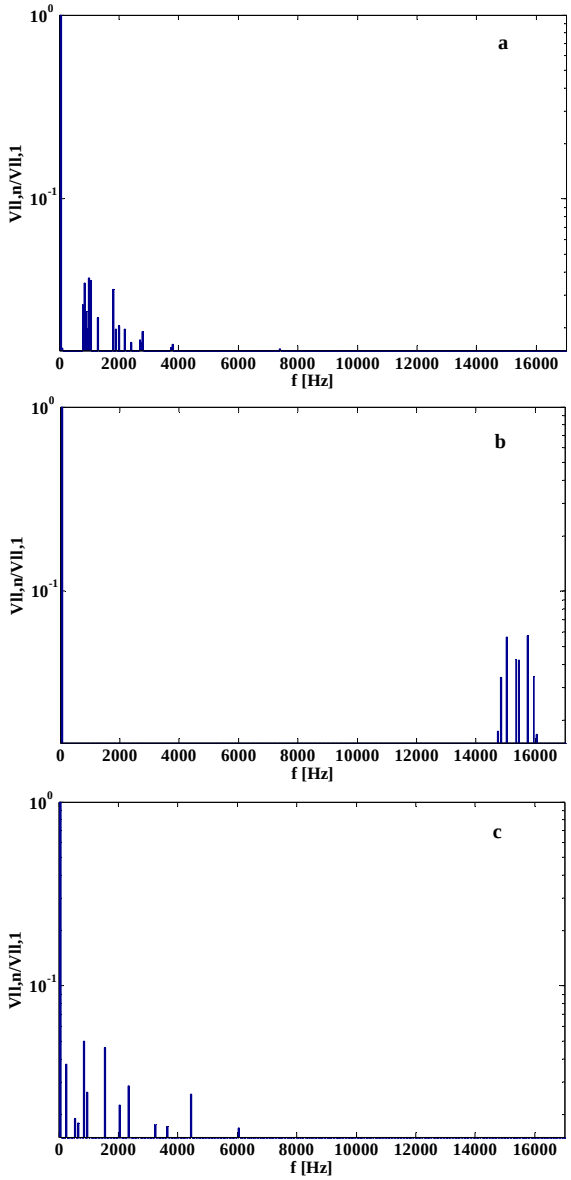

Figs. 8. Harmonic spectra of line-to-line voltage V_{ll} (I_{ph}=600A; f=50Hz; m_a=1.15) a) 5L-NPC(f_C=930Hz); b) 5L-SCHB(f_C=3850Hz); c) 5L-ASCHB(f_C=750Hz)

TABLE VIII
THD AND WTHD OF LINE-TO-LINE VOLTAGE; $f_C=f_{c,max}$

Topology	THD	WTHD
5L-NPC VSC	17.5 %	0.75 %
5L-SCHB VSC	23.7 %	0.05 %
5L-ASCHB VSC	17.5 %	0.77 %

IV.3. Loss Comparison with Constant S_s and f_{1cb}

In this section, a constant installed switch power (S_s = 47.89 MVA) as well as a constant frequency of the first carrier band are considered for all converter topologies. To center the first harmonics carrier band around the same frequency occurring at the 5L-SCHB VSC, the carrier frequencies of other topologies have to be tuned. This assumption enables the utilization of output filters with about the same sizes, costs and weights. The converter losses, the semiconductor loss distribution, and the harmonic spectra of topologies illustrated in Figs. 9-11.

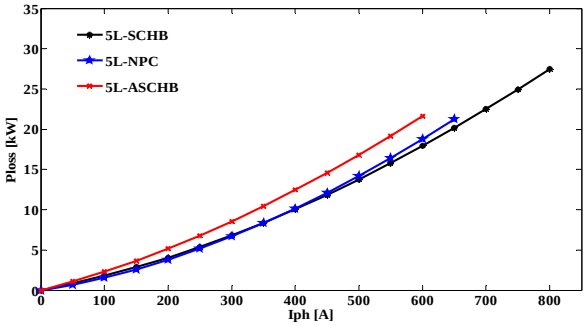

Fig. 9. Total converter losses as a function of phase current (f=50Hz; m_a=1.15; cosφ = 0.9)

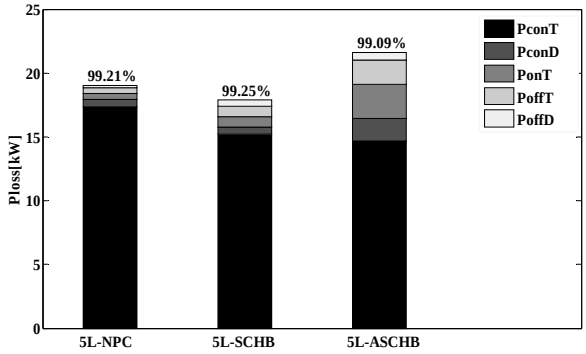

Fig. 10. Loss distribution of semiconductor and converter efficiency ($f_{C,5L\text{-}NPC}$=750Hz; $f_{C,5L\text{-}HB}$=188Hz; $f_{C,5L\text{-}AHB}$=750Hz; f=50Hz, m_a=1.15; cosφ = 0.9; I_{ph}=600A)

As shown in Fig. 9 the total losses of 5L-ASCHB is higher than other topologies in all ranges of output phase current. The maximum and minimum output powers achieve in the 5L-SCHB, and 5L-ASCHB VSCs respectively (Table IX). Also the first harmonics carrier band centered around 750 Hz (f_C) in both 5L-ASCHB, and 5L-NPC VSCs.

TABLE IX
MAXIMUM PHASE CURRENT AND APPARENT OUTPUT POWER FOR S_S=47.89 MVA; f_{1cb}=750 Hz; $T_{j,max}$=125 °C

Topology	5L-NPC VSC	5L-SCHB VSC	5L-ASCHB VSC	
Installed switch power (S_S)	47.89 MVA			
Frequency of the first harmonics carrier band (f_{1cb})	750 Hz			
Rated IGBT current ($I_{C,n}$)	626 A	782.5 A	Main	668 A
			Aux.	537 A
Carrier frequency (f_C)	750 Hz	750/4 Hz	750 Hz	
Maximum phase current ($I_{ph,max}$)	613 A	785 A	600 A	
Maximum apparent output power ($S_{C,max}$)	2.44 MVA	3.13 MVA	2.39 MVA	

There are many harmonic components at the 5L-SCHB VSC beyond a carrier frequency of 2500 Hz in comparison with other topologies as represented in Figs. 11. Therefore, the WTHD of 5L-SCHB VSC is higher than the 5L-NPC, and 5L-ASCHB VSCs (Table X).

V. Cost Comparison

The material costs at MV converters are relatively a dominant part of total converter cost (up to about 40%). Therefore, derive a detailed and complete comparison of the material costs of the considered components per MVA output power is necessary and would be performed. This section presents this comparison for the aforementioned topologies considering the component costs including the costs of the power semiconductor, the IGBT modules, diode modules, heat-sinks, and gate-drive units were obtained from the manufacturers for a device volume of 1000 devices per year. For comparison the water-cooled heat-sink Eupec KW51 (R_{thh-a} = 6 K/kW at a water flow rate of v_w = 6.2 L/min) was used throughout this paper (Table XI). To evaluate the real cost comparison, two important cost criteria (the converter switch utilization and the active silicon area for a specified output power) will be compared. The switch utilization is the ratio between S_C and S_S and related to the installed switch power and converter output power. The 5L-SCHB enables the highest output power with respect to its installed switch power. The active silicon area per MVA is the second important criteria. The 5L-SCHB achieve to the lowest active silicon area with respect to its output power compared to other topologies. The semiconductor costs comparison show that the 5L-ASCHB IGBTs module is more expensive than two other topologies. The cost comparison of the gate units and heat-sinks indicate that the 5L-ASCHB yields about 31% and 5% lower cost in comparison with 5L-NPC and 5L-SCHB VSCs respectively. The capacitor size and cost is strongly related to the amount of the stored energy in the dc-link. Then, considering a constant stored energy in the dc-link capacitor, the size and cost of dc-link capacitor will be almost the same for all considered topologies.

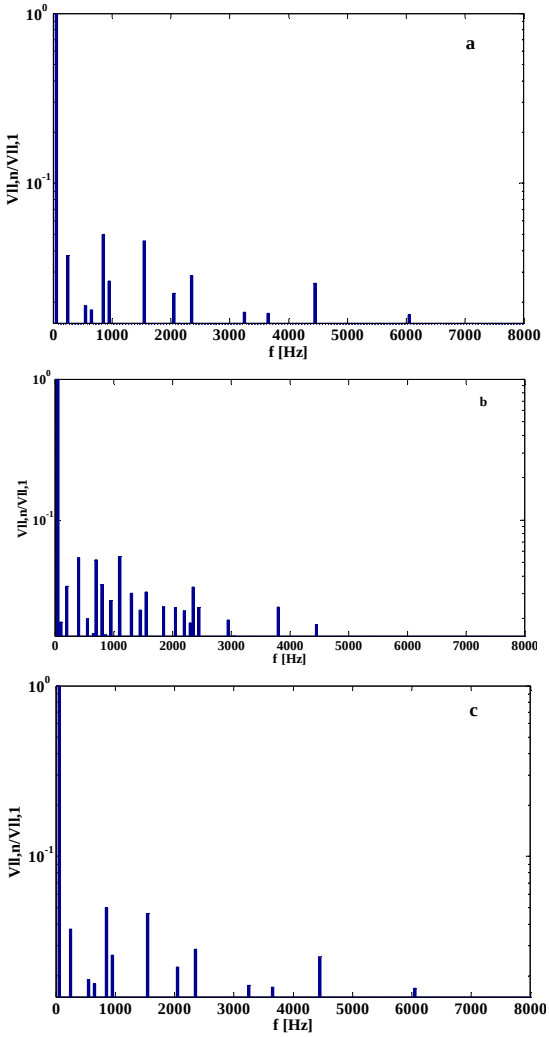

Figs. 11. Harmonic spectra of line-to-line voltage V_{ll} (f=50Hz, m_a=1.15); a) 5L-NPC(f_c=750Hz); b) 5L-SCHB(f_c=188Hz); c) 5L-ASCHB(f_c=750Hz)

TABLE X
THD AND WTHD OF LINE-TO-LINE OUTPUT VOLTAGE; $f_{C,5L-NPC}$=750Hz; $f_{C,5L-SCHB}$=375Hz; $f_{C,5L-ASCHB}$=750Hz; m_a=1.15

Topology	THD	WTHD
5L-NPC VSC	17.5 %	0.77 %
5L-SCHB VSC	23.7 %	1.26 %
5L-ASCHB VSC	17.5 %	0.77 %

TABLE XI
THE NUMBER AND UNIT PRICES OF THE 5 LEVEL TOPOLOGIES

Topology	5L-NPC	5L-SCHB	5L-ASCHB	
IGBT module footprint area	106.4*61.4 mm^2 (1.7 kV)	106.4*61.4 mm^2 (1.7 kV)	Main	140*130 mm^2 (3.3 kV)
			Aux.	106.4*61.4 mm^2 (1.7 kV)
Cost of IGBT module	6000 € (24 modules/1.7 kV)	6000 € (24 modules/1.7 kV)	7800 € (12 modules/3.3 kV)	
Cost of NPC diode module	1350 € (9 modules/1.7 kV)	0	0	
Cost of auxiliary IGBT module	0	0	750 € (3 modules/1.7 kV)	
Cost of auxiliary diode module	0	0	900 € (6 modules/1.7 kV)	
Cost of gate-drive for 1.7 kV IGBT/Diode	2280 €	2280 €	285 €	
Cost of gate-drive for 3.3 kV IGBT/Diode	0	0	1512 €	
Cost of heat-sink for 1.7 kV IGBT/Diode	6105 € (33 modules)	4440 € (24 modules)	1665 € (9 modules)	
Cost of heat-sink for 3.3 kV IGBT/Diode	0	0	2940 € (12 modules)	
Installed switch power (MVA)	46.85 (124%)	37.82 (100%)	47.89 (126%)	
Total cost	15735 € (124%)	12720 € (100%)	15852 € (125%)	
$S_{C,max}$/ S_S	50.95 (80%)	63.27 (100%)	49.91 (79%)	
Active silicon area/ $S_{C,max}$	283	228	Main	390 (3.3 kV)
			Aux.	290 (1.7 kV)

VI. Conclusion

This paper compares three types of Five-Level voltage source converters (5L-NPC, 5L-SCHB, and 5L-ASCHB VSCs) on the basis of state-of-the-art 3.3kV, and 1.7kV IGBTs for a 2.3kV medium voltage converter. The design of the power semiconductors, the installed switch power, converter losses, the semiconductor loss distribution, the harmonic spectra and material costs are considered. For constant installed switch power and constant carrier frequency, the maximum output power in 5L-SCHB VSC increased by 27% and 24% higher than 5L-ASCHB VSC and 5L-NPC VSC respectively. Assuming constant installed switch power and constant converter output power the 5L-SCHB VSC create the highest possible carrier frequency because of uniform semiconductor loss distribution compared to other topologies. However, it should be noted, that the frequencies of the first carrier band are $f_{lcb} = f_C$ (5L-NPC VSC); $f_{lcb} = 4f_C$ (5L-SCHB VSC); and $f_{lcb} = f_C$ (5L-ASCHB VSC). Thus the 5L-SCHB topology enables a higher resulting frequency of the first carrier band and a substantially lower weighted THD compared to the other topologies. For a constant installed switch power and a fixed frequency of the first carrier band to f_{lcb}=750 Hz the converter output power of the 5L-SCHB , and 5L-NPC VSCs are increased by factors of 1.31 and 1.02 compared to the output power of the 5L-ASCHB VSC.

Appendix

The number of IGBT modules, NPC diode modules, auxiliary IGBT modules, gate-drives and heat-sink are listed in Table A1, which N is the number of line-to-line output voltage level.

TABLE A1
THE NUMBER AND UNIT PRICES OF THE N LEVEL TOPOLOGIES

Topology	NPC	SCHB	ASCHB
Number of IGBT module	6(N-1)	6(N-1)	3(N-1)
NPC diode module(2 diode/module)	3(N-2)	0	0
Number of auxiliary IGBT module	0	0	3(N-1)/4
Number of auxiliary diode module (2 diode/module)	0	0	3(N-1)/2
Number of gate-drive	6(N-1)	6(N-1)	15(N-1)/4
Number of heat-sink	3(3N-4)	6(N-1)	21(N-1)/4

References

[1] M. Marchesoni, M. Mazzucchelli, Multilevel converters for high power AC drives: A review, *in Proc. IEEE International Symposium Industry Electronics (ISIE'93)*, Budapest, Hungary, 1993, pp. 38-43.

[2] W. A. Hill, C. D. Harbourt, Performance of medium voltage multilevel inverters, *Conf. Proc. IEEE-IAS, 1999*, pp. 1186-1192.

[3] P. W. Hammond, Medium Voltage PWM Drive and Method, *U.S. Patent 5,625,545*, assigned to Halmar Robicon Group, April 1997.

[4] M. Ayadi, L. El M'barki, M. A. Fakhfakh, M. Ghariani and R. Neji, A Comparison of PWM Strategies for Multilevel Cascaded and Classical Inverters Applied to the Vectorial Control of Asynchronous Machine, *International Review of Electrical Engineering (IREE)*, vol. 5, n. 5 (Part A), Oct. 2010, pp 2106-2114.

[5] M. Calais, V. G. Agelidis, L. J. Borle, M. S. Dymond, A transformer less five level cascaded inverter based single phase photovoltaic system, *in Proc. IEEE Power Electron. Spec. Conf., June 2000*, Galway, Ireland, pp. 1173-1178.

[6] K. Opal, H. Abrams, P. Hammond, Low and medium voltage PWM AC/DC power conversion method and apparatus, *U.S. Patent 5,638,263*, June 1997.
[7] Z. Peng, J. W. McKeever, D. J. Adams, A power line conditioner using cascade multilevel inverters for distribution systems, *in Proc. IEEE Industry. Applications. Society. Conf., Oct. 1997*, pp. 1316-1321.
[8] F. Z. Peng, J. S. Lai, Dynamic performance and control of a static var generator using cascade multilevel inverters, *IEEE Trans. Industry. Applications, vol. 33*, June 1997, pp. 748-755.
[9] A. J. Visser, H. Du, T. Mouton, J. H. R. Enslin, Direct-coupled cascaded multilevel sag compensator, *in Proc. IEEE Power Electronics. Spec. Conf., June 2000*, Galway, Ireland, pp. 463-469.
[10] G. Joos, X. Huang, B. T. Ooi, Direct-coupled multilevel cascaded series VAR compensators, *in Proc. IEEE Industry Applications Society, Oct. 1997*, pp. 1608-1615.
[11] D. Krug, S. Bernet, S. Dieckerhoff, Comparison of State-of-the-Art Voltage Source Converter Topologies for Meduim Voltage Applications, *in Conf. Rec. IEEE-IAS Annu. Meeting, 2003*, pp. 168 – 175.
[12] D. Krug, M. Malinowski, S. Bernet Design and Comparison of Medium Voltage Multi-Level Converters for Industry Applications, *in Conf. Rec. IEEE-IAS Annu. Meeting, 2004*, pp. 781 – 790.
[13] G. Ceglia, V. Guzman, C. Sanchez, F. Ibanez, J. Walter, A New Simplified Multilevel Inverter Topology for DC–AC Conversion, *IEEE Trans. on Power Electronics, vol. 21*, Sep. 2006, pp. 1311-1319.
[14] G. Ceglia, V. Grau, V. Guzman, C. Sanchez, F. Ibanez, J. Walter, A new multilevel inverter topology, *5th IEEE International Caracas Conference on Devices, Circuits and Systems, Nov. 2004*, Caracas, pp. 212-218.
[15] R. Benachour, S. Latreche, M. E. H. Latreche and C. Gontrand, Non Linear Average Model of Switching Loss Using in a Virtual Prototyping , *International Review of Modelling and Simulations (IREMOS),* vol. 3, no. 5, Oct. 2010 (Part A), pp 759-766.
[16] S. Bernet, Leistungshalbleiter als Nullstromschalter in Stromrichtern mit weichen Schaltvorgängen, Aachen: Verlag Shaker, 1995.
[17] T. Brückner, The active NPC Converter for Medium Voltage Drives, Verlag Shaker, 2006.
[18] S. S. Fazel, *Investigation and Comparison of Multi-Level Converters for Medium Voltage Applications*, Ph.D. dissertation, Berlin Technical University, 2007.

Authors information

[1,2,3]Iran University of Science and Technology, Tehran, Iran.

Mehdi Niakinezhad was born in Iran in 1986. He received the B.Sc. degree in electronic engineering from The Babol Noshirvani University of Technology, I.R.I. in 2008. He is with railway school of the University of Science and Technology Tehran, Iran. His research interests include Power Electronics and Vector Control.

Mohammad Ali Akbari Baseri was born in Iran in 1985. He received the B.Sc. degree in electrical engineering from The Shiraz University of Technology, I.R.I. in 2008. He is with railway school of the University of Science and Technology Tehran, Iran. His research interests include Power Electronics and Power Quality.

Seyed Saeed Fazel was born in Iran in 1966. He received the M.Sc. degree from Iran University of Science and Technology, Tehran, Iran, in 1993, and the Ph.D. degree from Berlin University of Technology, Germany, in 2007, all in Electrical Engineering. He spent four years (1994-1998) as an Engineer with Jahad Daneshgahi Elm Va Sanat (JDEVS), and was involved in High Voltage Transformer-Rectifier in Electrostatic Precipitator applications. Since 1998, he has been an Assistant Professor at the Iran University of Science and Technology, Tehran, Iran. His research interests include Power Electronics, Medium Voltage Converter Topologies and Electrical Machines.

Akram Mehdipour was born in Iran in 1986. She received the B.Sc degree in electronic engineering from the Industrial university of Babol, I.R.I in 2008. Her research interests include Power electronics, industrial control and control engineering.

International Review on Modelling and Simulations (IREMOS)

(continued from outside front cover)

(continued on outside back cover)

Abstracting and Indexing Information:

Academic Search Complete - EBSCO Information Services
Cambridge Scientific Abstracts - CSA/CIG
Elsevier Bibliographic Database SCOPUS
Index Copernicus (Journal Master List): ***Impact Factor 6.55***

Autorizzazione del Tribunale di Napoli n. 78 del 1/10/2008

(continued from inside back cover)

(continued on Part B)

Praise Worthy Prize

This volume cannot be sold separately by Part B

1974-9821(201106)4:3;1-S